Numerical Simulation of Townsend Discharge, Paschen Breakdown and Dielectric Barrier Discharges

Napoleon Leoni; Hewlett Packard Laboratories, Palo Alto, CA. Bhooshan Paradkar, Mech. Eng. Department, UCSD, San Diego, CA.

Abstract

Practical understanding of electrical discharges between conductors or between conductors and dielectrics is instrumental for the development of novel charging devices for Digital Printing Applications. The work presented on this paper focuses on fundamental aspects related to the inception of electrical discharges and breakdown in the initial stages (few 100's of μs) to a detail hard to match with experimental techniques. Numerical simulations of 1-D Townsend and Dielectric Barrier Discharges (DBDs) are performed using a commercial Finite Element package (COMSOL). A combined fluid model for the electron and Ion fluxes is used together with a local field approximation on a 1-D domain comprised of Nitrogen gas. The renowned Paschen breakdown result is successfully predicted numerically. Results are shown for the transient Townsend discharge that leads to this breakdown offering insight into the positive feedback mechanism that enables it. These transient results show how impact ionization combined with cathode secondary emission generate increasing waves of positive ions that drift towards the cathode again self feeding the discharge process. The simulation is then extended to predict the nature of a DBD in the case of a single voltage pulse.

Introduction

Gas Discharge Physics has been a topic of rigorous investigation in the scientific community for more than a hundred years both from a fundamental and a practical point of view. Dielectric Barrier Discharges (DBDs) in particular have attracted considerable attraction in recent times mainly due to its numerous applications in modern day life[1] such as plasma display panels, pollution control, surface modification, plasma chemical vapor deposition, etc.

One such relevant application of DBDs is in the design of novel charging devices[6] for use in electrophotography as shown in fig. 1. Although the basic physics of DBDs are more or less clear, some of the issues are still under constant investigation. The relative role of various physical mechanisms such as secondary impact ionizations, field emission from cathode and photoionization are still not clear when the discharge length is on the order of micrometers, mainly due to experimental challenges. The numerical simulation in these cases is an useful tool[7] to address some of the fundamental questions still to be answered and also to validate the existing experimental data.

This work will first discuss the mathematical model used for our parallel electrode numerical simulations. The results of this model are validated by first performing a simulation for a uniform DC electric field (with parallel plate electrodes) for which the so called "Paschen Curve" is well defined. Finally the extension of this model to a DBD is discussed including the required modifications for the boundary conditions. All the simulations discussed here are performed in only one dimension (1-D).

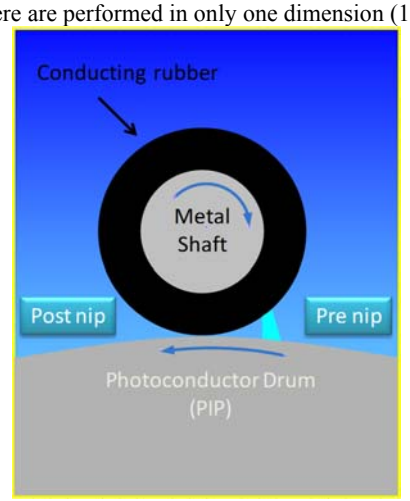

***Figure 1**. Example of DBD in a charge roller application in Digital Printing*

Numerical Model Definition

Nitrogen gas at atmospheric pressure is assumed as the working gas. The domain is one dimensional as shown in fig.2.

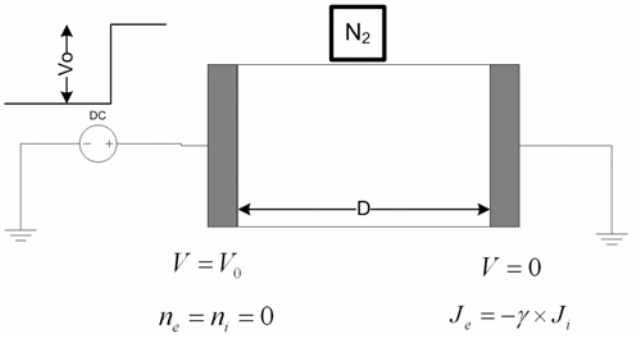

***Figure 2**. Numerical Model geometry and boundary conditions*

A hydrodynamic model [2] is used for the space charge flow together with a local field approximation model to allow computation of the transport coefficients, ionization coefficients and recombination coefficients as a function of the electric field to pressure ratio (E[V/cm]/p[Torr]). The governing Equations are shown below in terms of the local electrical potential (V), the

electron charge (e) and the ion (n_i) and electron(n_e) species concentration.

$$\frac{d^2V}{dx^2} = -\frac{e}{\varepsilon_0}\left(n_i - n_e\right) \ldots \text{Poisson equation} \quad (1)$$

$$\frac{\partial n_e}{\partial t} + \frac{\partial\left(n_e u_e - D_e \frac{\partial n_e}{\partial x}\right)}{\partial x} = G - L \ldots \text{electron continuity equation} \quad (2)$$

$$\frac{\partial n_i}{\partial t} + \frac{\partial\left(n_i u_i - D_e \frac{\partial n_i}{\partial x}\right)}{\partial x} = G - L \ldots \text{Ion continuity equation} \quad (3)$$

The continuity equations require knowledge of the diffusivity (D) and species drift velocity(u). Values for these variables where taken from [2] and [3]. Specifically we assumed D_e=1800 cm^2/s and D_i=0.046 cm^2/s. The electron and Ion drift velocities are calculated as shown in equations (4) and (5). The gain factor(G) and Loss factor(L) respectively represent the impact ionization (new electron ion-pairs) and recombination terms and are defined below as well in equations (6) and (7).

$$u_e = 2.9\times10^5 \frac{E}{p} \ldots \text{electron drift velocity} \quad (4)$$

$$u_i = 2.0\times10^3 \frac{E}{p} \ldots \text{ion drift velocity} \quad (5)$$

$$G = \alpha \cdot n_e u_e \ldots \text{impact ionization} \quad (6)$$

$$L = \beta \cdot n_e n_i \ldots \text{recombination} \quad (7)$$

$$\alpha = p\left[7.4326\times\exp\left(\frac{-270.5}{E/p}\right)\right] \ldots \text{ionization coefficient} \quad (8)$$

$$\beta = 2.0\times10^{-7} \ldots \text{recombination coefficient} \quad (9)$$

Boundary conditions at the electrodes are shown on fig. 2 in terms of the space charge fluxes at the wall (J) and the secondary emission coefficient γ =0.01. The space charge flux at the wall is defined generically as:

$$J_k = -\nabla\cdot(D_k n_k) + n_k u_k \ldots \text{space charge flux} \quad (10)$$

On equation (6) the index k may be replaced by "e" for electron or "i" for ion flux respectively. These boundary conditions physically mean that at the anode the surface charge is null, a reasonable assumption given that any charge landing on this surface will generate a counter image charge. At the cathode ion collisions generate free electrons at a rate of 1% of the incoming flux, this is surface and material dependent and the value assumed here is a typical figure [3].

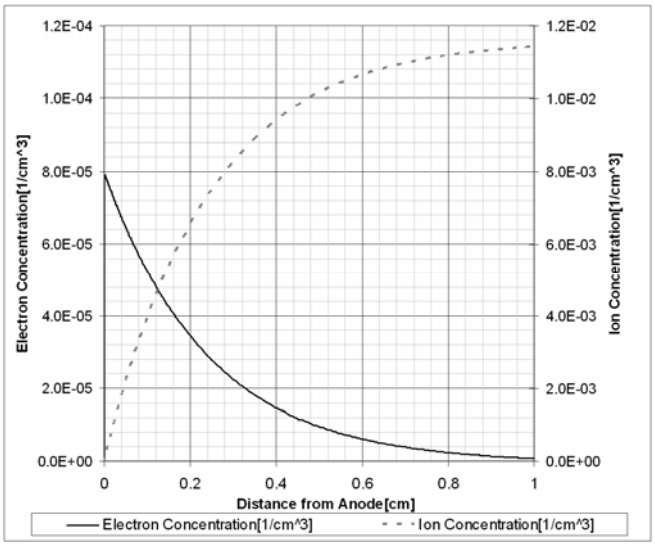

***Figure 3**. Steady state results for Ion and Electron concentration in domain*

Results and Discussion

Townsend discharge Prediction

The first simulation results shown on fig. 3 correspond to the steady state solution (solved through time evolution of the transient solution) for the electron and ion species concentration in our 1-D domain, basically the Townsend discharge regime between two parallel electrodes.

The specific conditions solved for in fig. 3 correspond to a gap of *D=1 cm* between the electrode and an applied potential of 28.5 kV. This value is close to the potential required for incipient breakdown. Note that the initial condition corresponds to 1000 ion-electron pairs/cm^3 in the domain so application of the field sweeps away most of this initial pairs, background electron-ion pair production provides a continuous source of charges supplemented with secondary emission from the cathode but the final result for this applied potential is still a net depletion of the original electron-ion pair population. Note the 100x factor between the electron and Ion concentration scales.

The effective space charge current density (A/cm^2) under these conditions may be calculated using the formula of Morrow and Sato[4]:

$$i(t) = \frac{e}{D}\int_0^D (-n_e u_e + n_i u_i)dx \ldots \text{discharge current} \quad (11)$$

This discharge current is computed for a given gap between the parallel electrodes as a function of the applied potential. The results for two different gaps (D=0.1 cm and D=1 cm) between the parallel electrodes are shown in fig. 4.

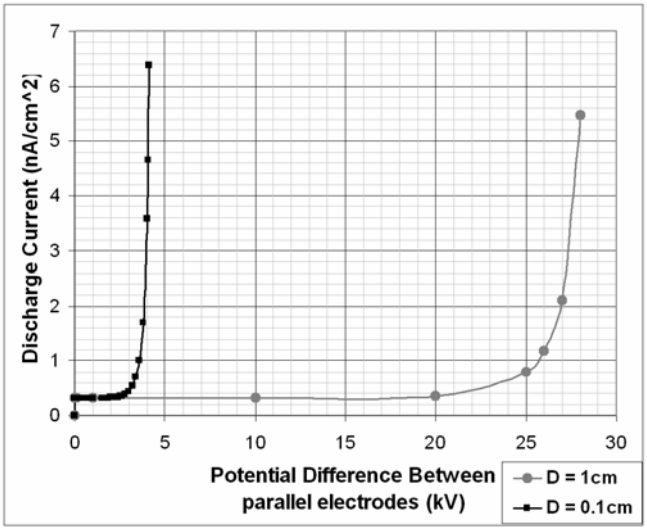

***Figure 4**. Discharge currents as a function of potential difference for two different spacing values between the parallel electrodes (D=0.1 cm and D= 1 cm)*

Casting the simulation results in the form of a discharge current as a function of the applied potential reveals two known characteristics of the Townsend discharge regime. First the existence of a constant current region in the curve which is interpreted as the current being limited by the background production of ion-electron pairs in the atmosphere, so in this regime the discharge is not self sustaining.

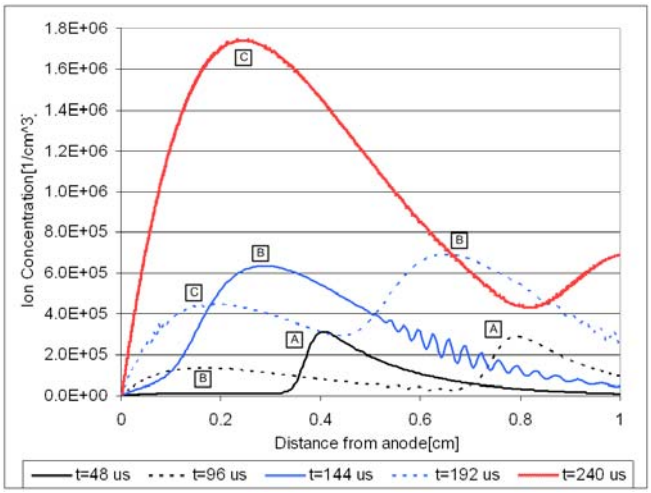

***Figure 5**. Transient results for Ion concentration in domain, traveling Ion waves*

As the potential is increased the current follows an exponential rise typically identified with incipient breakdown, here is where the simulation results are most valuable as we can study in detail the processes that yield this phenomena. Figure 5 shows the transient ion concentration distributions in our 1-D domain (*D=1 cm*) for different times after a potential of 30 kV has been applied. The initial condition is again the existing electron-ion pairs at atmospheric pressure (*~1000 pairs/cm^3* at *t=0*) due to cosmic ray induced ionization.

After the voltage is applied at time *t=0*, the electrons are swept very quickly towards the anode leaving evidence of their motion in the form of a peak in the space charge distribution of the ions due to impact ionization. This peak (denoted [A]) drifts towards the cathode at the expected ion drift speed also indicating a negligible space charge induced field. For reference u_i=*7.9x10^4 cm/s* for the applied field of *30 kV/cm* as computed from eq. (5). As this peak starts reaching the cathode a new secondary ionization induced electron wave is generated which generates a second peak [B] in the Ion concentration distribution.

Again the motion of this peak [B] is tracked on Fig. 5 as it drifts to the right towards the cathode. Each successive peak is larger than the previous one providing a positive feedback mechanism that leads to electrical breakdown. The oscillations displayed by some of the curves are probably numerical artifacts.

Note the concentration level for the Ion species in fig. 5 as compared to those of the steady solution in fig. 3, although the difference between the fields is small the compounding effect of the described positive feedback mechanism quickly yields a rise in the Ion concentration level of a 1000x the starting value.

Paschen Breakdown Prediction

Using the discharge current results from fig. 4 and computing these currents for different values of the gap *D* between the parallel electrodes we can generate the Paschen curve for Nitrogen. All what is needed is a criterion for the breakdown threshold. Ghaleb et al.[5] cite the criterion for Paschen discharge to be when the space charge concentration levels are 5.10^6 times the initial values. For building the Paschen curve below we have taken a somewhat arbitrary albeit meaningful threshold: a discharge current that is 10x the saturation current from the background electron-ion pair production. The computed Paschen curve is shown in fig. 6. The predicted Paschen curve displays the expected minimum ~340 V close to a 16 μm gap and the increased threshold for gaps smaller than this value.

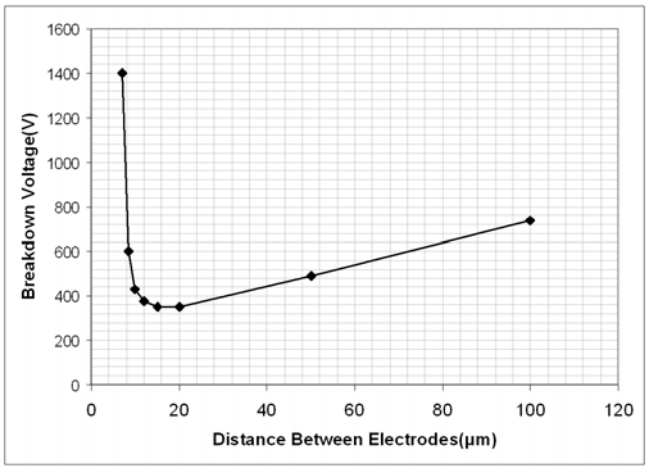

***Figure 6**. Numerical prediction of Paschen's Curve in Nitrogen*

DBD pulse numerical simulation

With added confidence on our numerical simulation we tackle next the problem of a DBD. As an example, the type of discharge that ensues between a charge roller and a photoimaging plate in an electrophotographic press is a DBD. The geometry under consideration is again 1-D and it is shown schematically in fig. 7. A single sinusoidal step of 2 kV is applied as shown with a rise time of 0.1 μs.

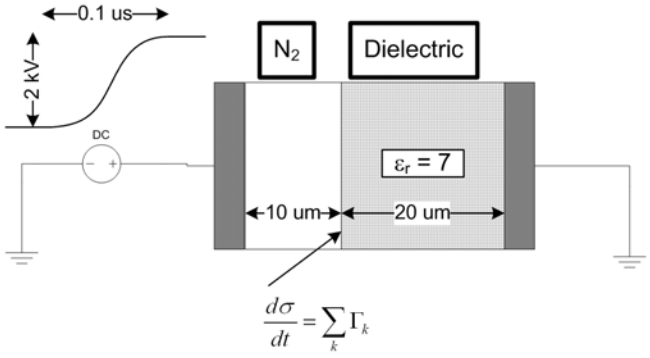

Figure 7*. DBD geometry and pulse excitation*

Boundary conditions are similar to those of fig. 2 with an additional boundary condition reflecting the accumulation of surface charge (σ) at the dielectric surface as the result of all the incoming space charge fluxes.

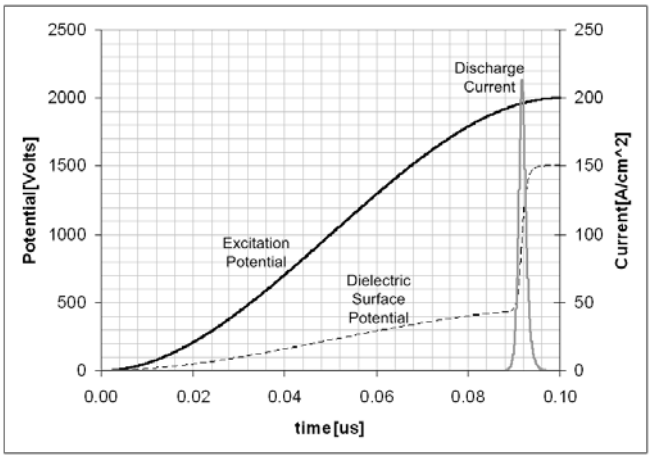

Figure 8*. DBD discharge current and dielectric charging as a result of a single pulse excitation*

Results for this DBD are given in fig. 8. Figure 8 shows three curves, the excitation potential applied between the electrodes, the surface potential on the dielectric and the discharge current. As the excitation potential is increased the threshold for a discharge is reached causing a pulse discharge lasting about 4 ns.

The charge carried by this pulse deposits on the dielectric increasing its potential and eventually quenching the discharge completely. This model could be extended to predict the charging behavior of a photoconductor plate and charge roller combination under different conditions.

Conclusion

A 1-D numerical model for Dielectric Barrier Discharges (DBDs) is presented. The model is first validated against the known "Paschen Curve" result showing the expected behavior at atmospheric pressure. Even for this simple parallel plate electrode geometry the numerical simulation provides insight on how secondary impact ionization at the cathode combined with impact ionization provide a positive feedback mechanism once the applied potential is above a threshold enabling the transition from the Townsend discharge regime to the Paschen Breakdown. Results for this transition between the Towsend discharge and breakdown are shown for a parallel plate electrode geometry with a 1 cm gap filled with Nitrogen gas and a 30 kV applied potential. The numerical model is then extended to a 1-D DBD in a 10 μm sized Nitrogen filled gap with a 20 μm dielectric (ε_r=7) solved for an applied step voltage of 2 kV (sinusoidal step with 100 ns rise time). The simulation allows prediction of the current discharge pulse that arises as the applied potential in the gap reaches the threshold value. The simulation also predicts the quenching of the barrier discharge as the dielectric surface is charged, effectively screening the applied potential.

References

[1] Ulrich Kogelschatz, Dielectric Barrier Discharges: Their History, Discharge Physics, and Industrial Applications, Plasma Chemistry and Plasma Processing, Vol. 23, No. 1, pg. 1 (2002)

[2] G E Georghiou et al, Numerical Modeling of atmospheric pressure gas discharges leading to plasma production, Journal of Physics D: Applied Physics, 38, pg. R303 (2005)

[3] E Panousis et al, Numerical Modeling of an atmospheric pressure dielectric barrier discharge in nitrogen: electrical and kinetic description, Journal of Physics D: Applied Physics, 40, pg. 4168 (2007)

[4] R Morrow and N Sato, The discharge current induced by the motion of charged particles in time-dependent electric fields; Sato's equation extended, Journal of Physics D: Applied Physics, 32, pg. L20 (1999)

[5] F. Ghaleb et al., Calculation of Breakdown voltage in plasma display panels, Materials Science and Engineering, 28, pg. 791 (2008)

[6] Omer Gila et al, High-Performance Charging Unit for Liquid Electrophotographic Presses, Proc. NIP 25: Int. Conf. on Digital Print. Tech., Loisville, KY(2009)

[7] H Kawamoto, Numerical Simulations of Electrophotography Processes, Plenary Talk, NIP 24, Int. Conf. on Digital Print. Tech., Pittsburgh, PA (2008)

Author Biography

Napoleon Leoni is a Mechanical Engineer in the Commercial Print Engine Lab of Hewlett Packard Laboratories. He received his B.Sc. Summa Cum Laude in Mechanical Engineering from Universidad Simon Bolivar in Venezuela in 1994 and his Ph.D. from Carnegie Mellon University in 1999. Prior to joining HP he worked on the development of nano-positioning systems for Disk Drive head testers. He joined HP in 2003 and has been working on developing novel charging systems for high speed digital presses.